Available online at www.sciencedirect.com

ScienceDirect

www.elsevier.com/locate/jprot

Global role of the membrane protease LonB in *Archaea*: Potential protease targets revealed by quantitative proteome analysis of a *lonB* mutant in *Haloferax volcanii*

Micaela Cerletti[a], *Roberto A. Paggi*[a], *Carina Ramallo Guevara*[b], *Ansgar Poetsch*[b,*], *Rosana E. De Castro*[a,*]

[a]*Instituto de Investigaciones Biológicas, Universidad Nacional de Mar del Plata (UNMDP), Consejo Nacional de Investigaciones Científicas y Técnicas (CONICET), Funes 3250 4to nivel, Mar del Plata (7600), Argentina*
[b]*Plant Biochemistry, Ruhr University Bochum, 44801 Bochum, Germany*

ARTICLE INFO

Article history:
Received 23 January 2015
Accepted 12 March 2015

Keywords:
LonB protease
Quantitative shotgun proteomics
Protein substrates
Phytoene synthase
Archaea
Haloferax volcanii

ABSTRACT

The membrane-associated LonB protease is essential for viability in *Haloferax volcanii*, however, the cellular processes affected by this protease in archaea are unknown. In this study, the impact of a *lon* conditional mutation (down-regulation) on *H. volcanii* physiology was examined by comparing proteomes of parental and mutant cells using shotgun proteomics. A total of 1778 proteins were identified (44% of *H. volcanii* predicted proteome) and 142 changed significantly in amount (≥2 fold). Of these, 66 were augmented in response to Lon deficiency suggesting they could be Lon substrates. The "Lon subproteome" included soluble and predicted membrane proteins expected to participate in diverse cellular processes. The dramatic stabilization of phytoene synthase (57 fold) in concert with overpigmentation of *lon* mutant cells suggests that Lon controls carotenogenesis in *H. volcanii*. Several hypothetical proteins, which may reveal novel functions and/or be involved in adaptation to extreme environments, were notably increased (300 fold). This study, which represents the first proteome examination of a Lon deficient archaeal cell, shows that Lon has a strong impact on *H. volcanii* physiology evidencing the cellular processes controlled by this protease in *Archaea*. Additionally, this work provides a platform for the discovery of novel targets of Lon proteases.

Biological Significance
The proteome of a Lon-deficient archaeal cell was examined for the first time showing that Lon has a strong impact on *H. volcanii* physiology and evidencing the proteins and cellular processes controlled by this protease in *Archaea*. This work will facilitate future investigations aiming to address Lon function in archaea and provides a platform for the discovery of endogenous targets of the archaeal-type Lon as well as novel targets/processes regulated by Lon proteases. This knowledge will advance the understanding on archaeal physiology and the biological function of membrane proteases in microorganisms.

* *Corresponding authors.*
E-mail addresses: ansgar.poetsch@ruhr-uni-bochum.de (A. Poetsch), decastro@mdp.edu.ar (R.E. De Castro).

http://dx.doi.org/10.1016/j.jprot.2015.03.016
1874-3919/

1. Introduction

Energy-dependent proteolysis maintains the quality of proteins and is used as a regulatory mechanism of cellular functions. Among the various proteolytic enzymes of the AAA+ (ATPases associated with diverse cellular activities) family that occur in bacteria and/or eukaryotes (ClpXP, ClpAP, ClpCP, HslUV, Lon, FtsH, PAN/20S, and the 26S proteasome) [1] only two are found in *Archaea*: a soluble 20S/PAN proteasome and a membrane-anchored LonB-type protease [2].

Proteasomes (which are present in *Eukarya*, Actinobacteria and *Archaea*) are involved in many processes of eukaryotic cells, including metabolism, DNA repair, cell division and antigen processing [3]. In the euryarchaeon *Haloferax volcanii* at least three proteasome sub-types have been identified [4]. As in eukaryotes, this proteolytic complex is essential for *H. volcanii* and is required for the stress response, protein quality control, cell division and other cellular functions [5,6].

Lon proteases are conserved across the three domains of life [7]. The LonA subfamily are soluble enzymes which function in the bacterial cytosol and the mitochondrial matrix. This subfamily has been extensively characterized and its biological relevance has been demonstrated in many organisms. With a few exceptions [8] Lon does not appear to be an essential protein under normal conditions. In most bacteria, however, it is required to remove abnormal proteins and regulates a myriad of cellular functions including the stress response, cell cycle and differentiation, motility, plasmid maintenance, sporulation as well as bacterial virulence [9]. Lon exerts multiple functions in human mitochondria including degradation of oxidized and carbonylated proteins, mtDNA replication and apoptosis [10]. It has been proposed that the accumulation of carbonylated proteins forms aggregates which are associated with the development of various age-related human disorders such as Parkinson and Alzheimer [11].

The LonB-subfamily is represented by membrane proteases and predominates in *Archaea*. Although the archaeal-type Lon homolog has been characterized biochemically and/or at the structural level in several archaea members [7], the physiological significance of this enzyme in the archaeal cell had not been explored until recently [12]. Whether the differential localization of this enzyme affects its function and/or substrate selectivity remains to be demonstrated.

Membrane-associated proteases are central in cell physiology as they perform quality control of membrane proteins and are involved in processing of exported polypeptides, regulatory circuits, cell-signaling, the stress response as well as the assembly of cell surface structures [13]. Most of the membrane proteases that occur in bacteria and eukaryotes are also encoded in archaeal genomes, except for the ATP-dependent metallo protease FtsH [2,7]. The biological role of some of these proteases in the context of archaeal cells (e.g. their relevance in the adaptation of these organisms to extreme habitats) is poorly understood.

Proteome analysis of wt vs protease-deficient strains evidences the impact that the protease exerts on the organism and helps in the discovery of potential protease substrates. Proteomics strategies have been applied in the bacterium *E. coli* to elucidate the biological function of the ClpP protease in stationary phase adaptation [14], and in virulence regulation of *Staphylococcus aureus* strains [15]. Similar strategies have facilitated the identification of novel protein substrates of the mitochondrial Lon protease [16–18]. Comparably, proteomics has been less applied to the study of membrane proteases and only a few natural substrates of these proteases have been identified. Some instances include the proteomic analysis of a *Corynebacterium glutamicum* FtsH protease mutant [19]; HtrA deletion mutants of *Bacillus anthracis* [20]; a proteomics-based substrate trapping approach to identify new FtsH substrates in *E. coli* [21]. In archaea, proteomics has been used to examine proteasome mutants of *H. volcanii* [22,23].

To gain insight on the biological role of the integral membrane LonB protease in archaea, we previously constructed mutant strains defective in Lon expression in the euryarchaeon *H. volcanii* and showed that this protease is essential for survival of this microorganism [12]. Sub-expression of Lon in a *lon* conditional mutant strain produced cell overpigmentation, increased the level of several lipids (including the C50 bacterioruberin carotenoids), affected growth, cell shape and antibiotic resistance. In *H. volcanii* (and other haloarchaea) the *lon* gene (HVO_0783) appears to form an operon with a sequence encoding a hypothetical protein related to the CAAX family of prenyl peptidases (HVO_0784) denoted by us as Abi [24]. To examine the potential contribution of this gene product in the phenotypes observed in the *lon* conditional mutant, a strain with a deletion in the coding sequence for *abi* [12] was constructed. So far, this strain has not evidenced differences compared to the wt, at least under the conditions tested.

In this study, proteomes of wt and a *lon-abi* conditional mutant were compared by quantitative high-throughput proteomics in order to understand the global impact of the LonB protease on archaeal physiology and to discover its potential protein substrates. This study expands the current knowledge on the biology of membrane proteases in microorganisms, a subject that remains scarcely explored.

2. Materials and methods

2.1. Strains and culture conditions

H. volcanii H26 wt and the mutant strain HVLON3 were used for proteome comparison. HVLON3 is a conditional expression strain which has the tryptophanase gene tryptophan-regulated promoter (P*tnaA*) [25] located upstream the *lon* gene in *H. volcanii* H26 chromosome (P*tnaA-lon-abi*). This strain synthesizes very low amounts of Lon and Abi in absence of trp in the culture medium [12]. As a control, the proteome of the strain HVABI, a deletion mutant of the downstream gene *abi* (Δ*abi*) [12] was analyzed in parallel and compared to that of the wt strain. To obtain the "Lon subproteome", proteins that changed as a consequence of the Abi mutation were discarded. These strains were grown in minimal medium (Hv-Min) containing uracil (50 μg ml^{-1}) [26] in absence of trp at 42 °C 200 rpm. Cell growth was monitored by measuring the optical density of the cultures at 600 nm (OD_{600}). Samples were taken at exponential (Exp) (OD_{600} ~ 0.5) and stationary (St) (OD_{600} ~ 1.5) growth phases. For proteome analysis four

independent cultures (biological replicates) of each strain were analyzed and compared.

2.2. Preparation of cytoplasm and membrane fractions

Cells were harvested by centrifugation (10000×*g*, 10 min, 4 °C), suspended in 100 mM HCl–Tris (pH 7.5) containing 2 M NaCl and disrupted with an ultrasonic processor (3 × 30 s, 80 W). Cell lysates were clarified by centrifugation (10000×*g*, 10 min, 4 °C) and the membranes pelleted (100000×*g*, 2 h, 4 °C) and washed with the same buffer (100000×*g*, 30 min, 4 °C). The membranes were suspended in 1/3 of the same buffer (~1 ml). To eliminate salts, cytoplasm and membrane proteins were precipitated overnight with 100% (v/v) acetone at 4 °C followed by centrifugation. The precipitated proteins were washed three times with 80% and once with 100% acetone and left to dry for a few minutes at room temperature.

2.3. Electrophoresis in polyacrylamide gels (SDS-PAGE)

Cytoplasm and membrane proteins were suspended in 1X Laemmli sample buffer (12 mM Tris–HCl pH 6.8, 0.4% (w/v) SDS, 0.02% (w/v) bromophenol blue (BPB), 0.1 M DTT, 5% (v/v) glycerol), incubated at 37 °C for 3 h (550 rpm) and loaded onto 10% (v/v) polyacrylamide gels containing 0.1% SDS (~30 μg per lane). The gels were run at room temperature until samples passed the stacking gel and all proteins were concentrated into one protein band in the separation gel. Proteins were visualized with a coomassie brilliant blue (CBB-G250) stain as described by Dyballa and Metzger (2009) [27].

2.4. In-gel tryptic digestion

Protein bands were excised from the gels and cut into small cubes (ca. 1 × 1 mm) which were completely destained according to Schluesener and colleagues (2005) [28]. Gel pieces were dried in a SpeedVac, trypsin (porcine, sequencing grade, Promega) solution (12.5 ng ml^{-1} in 25 mM ammonium bicarbonate, pH 8.6) was added until gel pieces were immersed completely in digestion solution. The protein digestion was performed overnight at 37 °C with agitation (tempered shaker HLC MHR20, 550 rpm). After digestion, elution buffer (50% acetonitrile, 0.5% TFA, UPLC grade, Biosolve, Netherlands) was added (1 μl elution buffer for each μl of digestion buffer) and the samples were sonicated for 20 min in an ultrasonic bath. The samples were centrifuged and the supernatants were transferred to new 1.5 ml tubes. The extracted peptides were dried using a SpeedVac and stored at −20 °C. Before MS-analysis peptides were re-suspended in 20 μl of buffer A (0.1% formic acid in water, ULC/MS, Biosolve, Netherlands) by sonication for 10 min and transferred to LC-MS grade glass vials (12 × 32 mm glass screw neck vial, Waters, USA). Each measurement was performed with 8 μl of sample.

2.5. One-dimensional nLC-ESI-MS/MS

An UPLC HSS T3 column (1.8 μm, 75 μm × 150 mm, Waters, Milford, MA, USA) and an UPLC Symmetry C_{18} trapping column (5 μm, 180 μm × 20 mm, Waters, Milford, MA, USA) for LC as well as a PicoTip Emitter (SilicaTip, 10 μm i.d., New Objective, Woburn, MA, USA) were used in combination with the nanoACQUITY gradient UPLC pump system (Waters, Milford, MA, USA) coupled to a LTQ Orbitrap XL (analysing the cytoplasm samples) or a LTQ Orbitrap Elite (analysing the membrane samples) mass spectrometer (Thermo Fisher Scientific Inc., Waltham, MA, USA). For elution of the peptides a linear gradient with increasing concentration of buffer B (0.1% formic acid in acetonitrile, ULC/MS, Biosolve, Netherlands) from 1% to 40% within 165 min was applied, followed by a linear gradient from 40% to 99% acetonitrile concentration within 15 min (0–5 min: 1% buffer B; 5–10 min: 5% buffer B; 10–165 min: 40% buffer B; 165–180 min: 99% buffer B; 180–195 min: 1% buffer B) at a flow rate of 400 nL min^{-1} and a spray voltage of 1.5–1.8 kV. The column was re-equilibrated at 1% buffer B within 15 min. The analytical column oven was set to 55 °C and the heated desolvation capillary was set to 200 °C (XL) or 275 °C (Elite). The LTQ XL Orbitrap was operated by instrument method files of Xcalibur (Rev. 2.0.7) and the LTQ Orbitrap Elite via instrument method files of Xcalibur (Rev. 2.1.0) in positive ion mode. The linear ion trap and Orbitrap were operated in parallel, i.e. during a full MS scan on the Orbitrap in the range of 300–1600 *m/z* (XL) or 150–2000 *m/z* (Elite) at a resolution of 60000 MS/MS spectra of the 10 most intense precursors, from most intense to least intense, were detected in the ion trap. All samples were re-analysed, but with reverse order of the 10 most intense precursor fragmentations, i.e. from least intense to most intense. All the measurements in the Orbitrap Elite were performed with the lock mass option (lock mass: *m/z* 445.120025) for internal calibration [29]. The relative collision energy for collision-induced dissociation (CID) was set to 35%. Dynamic exclusion was enabled with a repeat count of 1 and 60 seconds (XL) or 45 seconds exclusion duration window (Elite). Singly charged and ions of unknown charge state were rejected from MS/MS.

2.6. Protein identification and quantification

Protein identification was performed by SEQUEST [30] and MS Amanda [31] algorithms embedded in Proteome Discoverer 1.4 (Thermo Electron © 2008–2012) searching against the complete proteome database of *H. volcanii DS2* containing 4035 entries exported from the Halolex database [32] on 9/24/2013. The mass tolerance for precursor ions was set to 15 ppm (XL) or 7 ppm (Elite); the mass tolerance for fragment ions was set to 0.4 Da. Only tryptic peptides with up to two missed cleavages were accepted and the oxidation of methionine was admitted as a variable peptide modification. The false discovery rate (FDR) was determined with the percolator validation in Proteome Discoverer 1.4 and the q-value was set to 1% [33]. For protein identification the mass spec format-(msf)-files were filtered with peptide confidence “high” and two unique peptides per protein. Additionally protein grouping options were enabled as default, which means consider only PSMs with confidence at least “medium” and consider only PSMs with delta CN better than 0.15. The complete set of results from the Proteome Discoverer searches can be found in Supplemental Tables S3(1–4) in [34]. Proteins were quantified by spectral counting [35,36] and a protein was considered as significantly regulated at a log2 value of at least 1 and −1 (2-fold) and $p < 0.05$ (Student’s t-test). Only proteins that had on average at least 5 PSMs (peptide scoring mass spectrum matches) were taken into consideration.

3. Results and discussion

3.1. Global analysis of total proteins identified in *H. volcanii* parent and lon mutant strains

To evaluate the relevance of the LonB protease in the physiology of archaeal cells, the proteomes of the parent *H. volcanii* H26 and the conditional mutant (HVLON3) were compared at different growth stages. Based on the standards indicated in Materials and methods section, a total of 1778 proteins were detected including membrane and cytoplasm fractions (see Supplemental Table S1 in [34]), which represents 44% of the predicted proteome of *H. volcanii*. Fig. 1A shows the distribution of the identified proteins in both strains (wt and HVLON3) at different growth stages. Unique proteins detected in each condition are shown in Supplemental Table S2 in [34]. These proteins were classified into different functional categories according to the HaloLex Database (Fig. 1B). Of the proteins identified in the membrane fraction, 37% were predicted to be membrane-associated or secreted, based on the presence of signal peptides and/or transmembrane domains. The remaining proteins may be associated to the membrane by other means (e.g. other protein/s) or may result from contamination with the cytoplasm.

3.2. Proteins showing differential abundance between the parent and Lon deficient strain

In agreement with its predicted localization, LonB was detected in the membrane proteome of the wt and HVLON3 mutant and, in the latter strain, the protein level of Lon was significantly down-regulated to about 5-fold (Table 1). In contrast, Abi was not detected in either strain probably due to the fact that polypeptides with various hydrophobic transmembrane domains are frequently underrepresented in tryptic digests [37].

Out of the proteins that were found to be differentially represented between the parent and the HVLON3 strain, 142 (65 from the membrane, 72 from the cytosol and 5 from both fractions) changed by ≥ 2 fold (Table 1) and were attributed to Lon deficiency based on comparison with the subproteome of a Δ*abi* strain. Of these, 66 proteins increased their concentration in the mutant cells, thus, they could represent potential natural substrates of the LonB protease. In addition, this group may also contain proteins indirectly controlled by Lon as well as those induced as a consequence of the stress generated by accumulation of abnormal proteins. In contrast, 77 proteins decreased their concentration suggesting that their synthesis may be indirectly stimulated by Lon (e.g. by degradation of a repressor protein).

The "Lon subproteome" composition was growth phase-dependent: 28 proteins varied their concentration in the Exp phase, 99 in the St phase, while 15 changed in both growth phases (Fig. 2). This means that even though the Lon protein concentration was similarly suboptimal at different growth stages (down-regulated 4.9 and 3.8 fold in Exp and St phase, respectively) (Table 1), Lon activity and/or substrate selection appears to be controlled in a growth phase-dependent manner. At the same time, this outcome suggests that LonB seems to be particularly important in controlling the level of regulatory

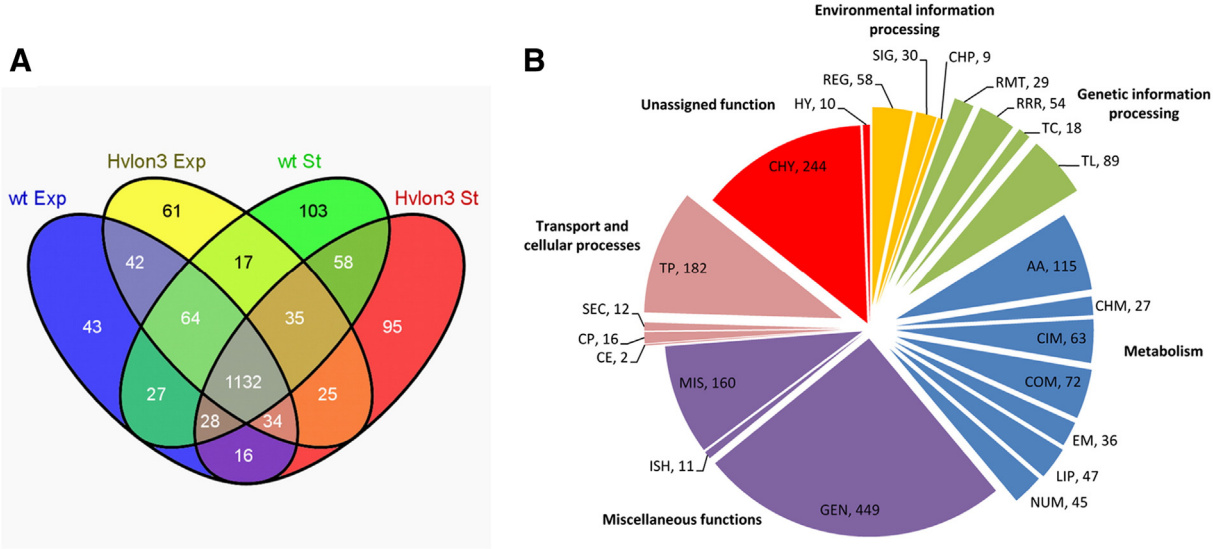

Fig. 1 – Distribution of total proteins identified in *H. volcanii* wt and HVLON3 strains. Protein detection was based on a minimum of two unique peptides (in at least one biological replicate) with a minimal false discovery rate of q-value ≤ 1%. A. Venn diagram [68] showing the distribution of identified proteins in both strains and growth stages. Several proteins were found to be unique for each condition (see Supplemental Table 2 in [34]). B. Classification into functional categories according to HaloLex Database. REG: gene regulation, SIG: signal transduction, CHP: chaperones, RMT: RNA maturation, RRR: replication, repair, recombination, TC: transcription, TL: translation, AA: amino acid metabolism, CHM: carbohydrate metabolism, CIM: central intermediary metabolism, COM: coenzyme metabolism, EM: energy metabolism, LIP: lipid metabolism, NUM: nucleotide metabolism, GEN: general enzymatic function, ISH: transposases and ISH-encoded proteins, MIS: miscellaneous, CE: cell envelope, CP: cellular processes, SEC: protein secretion, TP: small molecule transport, CHY: conserved hypothetical protein, HY: hypothetical protein.

Table 1 – *H. volcanii* proteins that showed a significant change (≥2 fold) between a wt and a *lon* deficient strain. Regulation factors for four biological replicates were submitted to a Student's t-test and *p*-values ≤ 0.05 were considered significant. Changes are expressed in fold (positive and negative numbers signify an increase or decrease in the mutant strain, respectively). FR, cellular fraction in which the protein was found to be differential (C: cytoplasm, M: membrane); TM, transmembrane domains or signal peptides according to HaloLex (Sig: signal sequence cleavage site, TAT: TAT export signal prediction, RR: lipobox RRLAGC motif); FC, functional category (see Fig. 1 for references).

ID	FR	TM	FC	Gene name	Protein name	Fold Exp	*p*-value	Fold St	*p*-value
Environmental information processing									
HVO_0179	C	0	REG	*trh1*	Lrp/AsnC family transcription regulator/TrkA domain protein			**−5.1**	0.024
HVO_1552	M	2	REG		ArsR family transcription regulator	**−8.8**	0.050		
HVO_2108	C	0	REG	*arcR3*	IclR family transcription regulator			**−15.0**	0.001
HVO_2858	C	0	REG	*asnC*	Lrp/AsnC family transcription regulator			**11.7**	0.008
HVO_0420	M	2	SIG	*mpcT, htr14*	transducer protein MpcT			**−4.5**	0.038
Genetic information processing									
HVO_0180	C	0	RMT	*ftsJ, rlmE*	23S rRNA (uridine-2'-O-) methyltransferase	**11.7**	0.027		
HVO_1094	M	0	RMT	*rnp3*	ribonuclease P protein component 3			**−2.0**	0.015
HVO_1895	C	0	RMT	*kae1*	KEOPS complex subunit Kae1/Bud32			**−2.5**	0.005
HVO_2746	C	0	RMT	*ksgA*	ribosome biogenesis protein KsgA. 16S rRNA-methylating			**−2.4**	0.001
HVO_0029	C	0	RRR	*uvrB*	UvrABC system protein B			**−9.6**	0.045
HVO_0175	M	0	RRR	*pcnA*	DNA polymerase sliding clamp			**2.1**	0.021
HVO_1565	C	0	RRR	*ligA*	DNA ligase (ATP)			**−7.5**	0.047
HVO_0795	C	0	TC	*tfb6*	transcription initiation factor TFB			**−20.2**	0.013
HVO_0677	M	0	TL	*aspS*	aspartate–tRNA ligase	**1.3**	0.025	**2.0**	0.001
HVO_2554	C/M	0	TL	*rpl14*	50S ribosomal protein L14			**–15.5/-2.5**	0.001/0.049
HVO_2555	M	0	TL	*rps17*	30S ribosomal protein S17	**−1.4**	0.029	**−2.9**	0.031
HVO_2560	C	0	TL	*rps19*	30S ribosomal protein S19	**−14.3**	0.000		
HVO_2562	M	0	TL	*rpl23*	50S ribosomal protein L23			**−2.0**	0.022
HVO_2564	C	0	TL	*rpl3*	50S ribosomal protein L3	**−3.9**	0.003	**−40.3**	0.000
HVO_2782	M	0	TL	*rps11*	30S ribosomal protein S11			**−2.8**	0.011
Metabolism									
HVO_0148	M	0	AA	*ureC*	urease alpha subunit			**14.5**	0.005
HVO_0161	M	0	AA	*hisG*	ATP phosphoribosyltransferase			**12.5**	0.030
HVO_0792	M	0	AA	*aroB*	3-dehydroquinate synthase type II			**9.8**	0.007
HVO_1079	M	0	AA	*cysD1*	sulfate adenylyltransferase small subunit	**10.7**	0.036		
HVO_1097	C	0	AA	*dapF*	diaminopimelate epimerase			**−4.6**	0.001
HVO_1098	M	0	AA	*lysA*	diaminopimelate decarboxylase			**6.8**	0.044
HVO_1099	M	0	AA	*dapD*	2.3.4.5-tetrahydropyridine-2.6-dicarboxylate N-succinyltransferase			**3.3**	0.012
HVO_1100	M	0	AA	*dapB*	4-hydroxy-tetrahydrodipicolinate reductase			**25.6**	0.016
HVO_1295	M	0	AA	*hisC*	histidinol-phosphate aminotransferase			**16.7**	0.002
HVO_1370	M	0	AA	*proA*	gamma-glutamyl phosphate reductase			**2.0**	0.012
HVO_2946	C	0	AA	*metB2*	cystathionine synthase/lyase			**−6.6**	0.040
HVO_2999	C	0	AA	*metY1*	O-acetylhomoserine aminocarboxypropyltransferase (methionine synthase)			**−34.9**	0.000
HVO_C0077	C	0	AA	*soxA2*	sarcosine oxidase			**−2.2**	0.049
HVO_1500	C	0	CHM	*pfkB*	1-phosphofructokinase			**−14.6**	0.023
HVO_A0331	C	0	CHM	*dgoD1*	D-galactonate dehydratase			**−3.8**	0.021
HVO_1538	C	0	CIM	*glpA1*	glycerol-3-phosphate dehydrogenase subunit A			**−2.7**	0.046
HVO_1539	C	Sig	CIM	*glpB1*	glycerol-3-phosphate dehydrogenase subunit B			**−2.1**	0.006
HVO_A0328	C	0	CIM	*kdgK2*	2-keto-3-deoxygluconate kinase			**−12.4**	0.021
HVO_0974	C/M	0	COM	*ribH*	6.7-dimethyl-8-ribityllumazine synthase	**-/-8.4**	0.037	**40.3/-**	0.000
HVO_1088	M	0	COM	*folCP*	folylpolyglutamate synthase/7.8-dihydropteroate reductase/dihydropteroate synthase	**−3.8**	0.029		
HVO_1469	C	0	COM	*menD*	2-succinyl-5-enolpyruvyl-6-hydroxy-3-cyclohexene-1-carboxylate synthase			**−4.4**	0.037
HVO_1861	C	0	COM	*thiL*	thiamine-monophosphate kinase			**−11.9**	0.014
HVO_1878	C/M	0	COM	*nadE*	NAD synthase	**1.6/-**	0.040	**2.1/9.9**	0.007/0.032

(continued on next page)

Table 1 (*continued*)

ID	FR	TM	FC	Gene name	Protein name	Fold Exp	*p*-value	Fold St	*p*-value
HVO_1936	C	0	COM	*cofE*	F420-0:gamma-glutamyl ligase			**−9.4**	0.025
HVO_2227	C	0	COM	*ahbA, nirDL*	siroheme decarboxylase AhbA			**−35.6**	0.000
HVO_2304	M	0	COM	*moeA1*	molybdenum cofactor biosynthesis protein MoeA	**15.2**	0.008		
HVO_2703	M	0	COM	*panB2*	3-methyl-2-oxobutanoate hydroxymethyltransferase	**−2.1**	0.016		
HVO_A0487	M	0	COM	*cbiA, cobB*	cobyrinic acid a.c-diamide synthase	**11.4**	0.030		
HVO_B0051	M	0	COM	*hmcA*	ATP-dependent cobaltochelatase subunit ChlID	**2.5**	0.004		
HVO_B0054	C	0	COM	*cbiX1*	sirohydrochlorin cobaltochelatase	**9.8**	0.013		
HVO_B0057	M	0	COM	*cbiH2, cobJ2*	precorrin-3B C17-methyltransferase	**9.8**	0.047		
HVO_B0058	C	0	COM	*cbiH1, cobJ1*	precorrin-3B C17-methyltransferase	**27.0**	0.002		
HVO_0310	C	0	EM	*atpH*	A-type ATP synthase subunit H			**8.6**	0.038
HVO_0979	C	0	EM	*nuoB*	NADH dehydrogenase-like complex subunit B	**−2.0**	0.028		
HVO_0146	M	1	LIP	*psd*	phosphatidylserine decarboxylase			**−12.0**	0.039
HVO_0896	C	0	LIP	*acs2*	acyl-CoA synthetase			**−3.8**	0.018
HVO_1585	C	0	LIP	*acs5*	acyl-CoA synthetase			**−5.3**	0.001
HVO_2524	M	0	LIP	*crtB*	phytoene synthase (PS)	**50.7**	0.012	**57.3**	0.015
HVO_2716	C	0	LIP	*acd5*	acyl-CoA dehydrogenase			**−2.1**	0.015
HVO_2918	C	0	NUM	*hts*	thymidylate synthase			**−7.3**	0.035
Miscellaneous functions									
HVO_0100	C	0	GEN		NMD3 family protein			**−2.4**	0.016
HVO_0208	C	0	GEN	*guaAa2*	glutamine amidotransferase (homolog to GMP synthase subunit A)			**−13.9**	0.002
HVO_0721	M	0	GEN		PHP domain protein	**−3.2**	0.038		
HVO_0773	M	0	GEN	*pnm*	probable S-adenosylmethionine-dependent methyltransferase	**−1.5**	0.021	**−2.0**	0.038
HVO_0889	C	0	GEN		FAD-dependent oxidoreductase			**16.3**	0.035
HVO_1020	C	0	GEN		HEAT-PBS family protein			**−2.5**	0.040
HVO_1022	M	0	GEN		NamA family oxidoreductase (homolog to old yellow enzyme)			**5.1**	0.045
HVO_1184	M	1	GEN		DUF1511 family protein			**−3.0**	0.003
HVO_1241	M	TAT	GEN	*prrC*	SCO1/SenC/PrrC family protein	**2.2**	0.005		
HVO_1291	M	0	GEN	*hpcE*	fumarylacetoacetase family protein	**14.2**	0.042		
HVO_1377	C	0	GEN		UPF0145 family protein			**12.9**	0.000
HVO_1656	C	0	GEN		YyaL family protein			**−3.1**	0.036
HVO_1918	C	0	GEN		probable metallo-beta-lactamase family hydrolase			**−11.7**	0.043
HVO_1925	C	0	GEN	*gbp3*	probable GTP-binding protein			**−16.6**	0.016
HVO_2040	M	0	GEN	*galE4*	NAD-dependent epimerase/dehydratase	**1.9**	0.029	**2.8**	0.000
HVO_2127	C	0	GEN		M20 family amidohydrolase (homolog to indole-3-acetyl-aspartic acid hydrolase)			**−20.1**	0.024
HVO_2153	C	TAT/RR	GEN	*mcoA*	probable copper-containing oxidoreductase			**−4.2**	0.046
HVO_2229	C	Sig	GEN		flavin-containing amine-oxidoreductase			**−9.6**	0.021
HVO_2239	C	0	GEN	*uspA19*	UspA domain protein	**−2.5**	0.046		
HVO_2356	M	0	GEN		GNAT family acetyltransferase			**2.3**	0.030
HVO_2421	C	0	GEN		probable DNA-binding protein			**21.8**	0.000
HVO_2606	M	0	GEN		PQQ repeat protein	**2.3**	0.026	**−0.6**	0.015
HVO_2607	M	TAT	GEN		PQQ repeat protein			**2.3**	0.000
HVO_2665	M	0	GEN	*hpcH*	HpcH/HpaI aldolase family protein			**5.4**	0.003
HVO_2670	M	0	GEN		FAD-dependent oxidoreductase (GlcD/DLD_GlcF/GlpC domain fusion protein)			**−2.1**	0.006
HVO_2932	C	0	GEN	*gbp4*	GTP-binding protein			**−27.5**	0.000
HVO_A0088	M	0	GEN		FAD-dependent oxidoreductase (GlcD/DLD_GlcF/GlpC domain fusion protein)			**−2.2**	0.005
HVO_A0268	C	0	GEN	*fuca*	class II aldolase (homolog to L-fuculose-phosphate aldolase)			**−10.2**	0.032
HVO_A0472	C/M	0	GEN	*trxB6*	oxidoreductase (homolog to thioredoxin-disulfide reductase)			**2.1/2.0**	0.021/0.001
HVO_A0547	C	0	GEN		DUF1028 family protein	**2.1**	0.020	**1.8**	0.048
HVO_B0052	C	0	GEN		PQQ repeat protein	**2.9**	0.007		
HVO_B0070	M	0	GEN	*gabT1*	pyridoxal phosphate-dependent aminotransferase	**−4.0**	0.040		

Table 1 (*continued*)

ID	FR	TM	FC	Gene name	Protein name	Fold Exp	*p*-value	Fold St	*p*-value
HVO_B0111	C	0	GEN		homolog to mandelate racemase/homolog to muconate lactonizing enzyme			**−12.5**	0.007
HVO_C0067	C	0	GEN	*soxA3*	FAD-dependent oxidoreductase			**−2.3**	0.002
HVO_0001	C	0	MIS	*orc1*	Orc1-type DNA replication protein			**−8.1**	0.011
HVO_0165	M	0	MIS	*mtaD*	5-methylthioadenosine/S-adenosylhomocysteine deaminase			**15.0**	0.029
HVO_1212	M	0	MIS	*cirA*	KaiC-type circadian regulator CirA			**2.1**	0.004
HVO_1257	M	0	MIS	*moxR2*	AAA-type ATPase (MoxR subfamily)			**2.3**	0.007
HVO_1523_A	M	2	MIS	*aglE*	glycosyltransferase AglE			**−2.6**	0.035
HVO_1648	C	0	MIS	*cyaB*	adenylate cyclase			**11.7**	0.001
HVO_1987	M	Sig	MIS	*sppA2*	signal peptide peptidase			**77.7**	0.010
HVO_2269	C	0	MIS	*rmeR*	type I site-specific deoxyribonuclease subunit RmeR			**−2.1**	0.020
HVO_A0257	C	0	MIS	*orc7*	Orc1-type DNA replication protein			**−9.2**	0.009
HVO_B0001	C	0	MIS	*orc6*	Orc1-type DNA replication protein			**−3.7**	0.003
HVO_B0371	C	0	MIS	*aldH1*	aldehyde dehydrogenase			**−2.4**	0.020
Transport and cellular processes									
HVO_0783	M	2	CP	*lon*	ATP-dependent protease La	**−4.9**	0.001	**−3.8**	0.001
HVO_2923	C	0	CP	*psmA2*	proteasome alpha subunit	**1.9**	0.021		
HVO_B0118	M	0	CP	*sph2*	SMC-like protein Sph2			**2.3**	0.012
HVO_0534	C	0	TP	*tsgD1*	ABC-type transport system ATP-binding protein (probable substrate sugar)			**−6.6**	0.049
HVO_0564	M	TAT	TP	*malE*	ABC-type transport system periplasmic substrate-binding protein (probable substrate maltose)			**−2.0**	0.021
HVO_0627	C	0	TP	*dppDF2*	ABC-type transport system ATP-binding protein (probable substrate dipeptide/oligopeptide)	**82.9**	0.000		
HVO_0891	M	0	TP	*nosF*	ABC-type transport system ATP-binding protein (probable substrate copper)			**24.5**	0.008
HVO_0899	M	TAT	TP	*livJ1*	ABC-type transport system periplasmic substrate-binding protein (probable substrate branched-chain amino acids)			**−31.6**	0.012
HVO_2163	M	0	TP	*lolD*	ABC-type transport system ATP-binding protein (homolog to LolDCE lipoprotein release factor)	**1.9**	0.003	**1.8**	0.022
HVO_2165	M	0	TP	*lolE*	ABC-type transport system permease protein (homolog to LolDCE lipoprotein release factor)			**6.8**	0.021
HVO_2800	M	0	TP	*livF3*	ABC-type transport system ATP-binding protein (probable substrate branched-chain amino acids)	**2.1**	0.046		
HVO_A0477	M	TAT	TP	*pstS2*	ABC-type transport system periplasmic substrate-binding protein (probable substrate phosphate)	**14.6**	0.006		
HVO_A0494	M	TAT/RR	TP	*tsgA6*	ABC-type transport system periplasmic substrate-binding protein (probable substrate sugar)			**−1.9**	0.020
HVO_B0021	M	TAT	TP	*dppA10*	ABC-type transport system periplasmic substrate-binding protein (probable substrate dipeptide/oligopeptide)			**−65.0**	0.014
HVO_B0047	C	0	TP		ABC-type transport system periplasmic substrate-binding protein (probable substrate iron-III)	**−8.9**	0.044		
Unassigned function									
HVO_0402	C	0	CHY		DUF124 family protein			**2.0**	0.027
HVO_0407	C	0	CHY		conserved hypothetical protein			**21.9**	0.000
HVO_0583	M	0	CHY		conserved hypothetical protein			**−12.3**	0.047
HVO_1134	C/M	0	CHY		conserved hypothetical protein	**1.9**/**3.3**	0.000/0.040	**2**/-	0.013
HVO_1240	M	TAT/RR	CHY		conserved hypothetical protein			**2.4**	0.007
HVO_1332	C	0	CHY		conserved hypothetical protein			**2.4**	0.001
HVO_1564	C	0	CHY		conserved hypothetical protein			**−8.0**	0.029
HVO_1577	M	0	CHY		conserved hypothetical protein			**6.4**	0.019
HVO_1812	C	0	CHY		conserved hypothetical protein			**−21.4**	0.000
HVO_1988	M	Sig	CHY		conserved hypothetical protein			**122.2**	0.000
HVO_2047	M	0	CHY		conserved hypothetical protein			**−2.0**	0.016
HVO_2519	M	0	CHY		conserved hypothetical protein			**4.2**	0.035
HVO_A0133	C	TAT	CHY		conserved hypothetical protein			**−14.5**	0.042

(*continued on next page*)

Table 1 (*continued*)

ID	FR	TM	FC	Gene name	Protein name	Fold Exp	*p*-value	Fold St	*p*-value
HVO_A0350	C	TAT	CHY		conserved hypothetical protein	**25.6**	0.005		
HVO_A0406	M	0	CHY		conserved hypothetical protein	**3.6**	0.014		
HVO_A0418	C	0	CHY		conserved hypothetical protein			**16.5**	0.000
HVO_A0432	M	0	CHY		conserved hypothetical protein	**3.6**	0.011		
HVO_A0476	C	0	CHY		conserved hypothetical protein			**−13.3**	0.016
HVO_A0627	M	TAT/RR	CHY		conserved hypothetical protein	**1.9**	0.038		
HVO_B0055	C	0	CHY		conserved hypothetical protein			**2.0**	0.031
HVO_A0012	C	0	HY		hypothetical protein	**21.7**	0.000	**19.0**	0.004
HVO_A0039	M	1	HY		hypothetical protein	**321.3**	0.000	**94.8**	0.016

and/or metabolic proteins in the St phase (and probably under other stress conditions) similarly as in bacteria [9].

The proteins differentially represented in cells with suboptimal Lon content (Table 1) are predicted to participate in various cellular processes, the most relevant being metabolism (lipids, amino acids and coenzyme biosynthesis), genetic processes and solute transport (Fig. 2). Additionally, there were many proteins of so far unknown function that were affected by Lon down-regulation, some of which were dramatically enriched, e.g. HVO_A0039 (321 fold) and HVO_1988 (122 fold).

Altogether, these results show that the LonB protease has a global impact on *H. volcanii* physiology affecting key cellular processes in metabolically active cells (ribosome stability, biosynthetic pathways) as well as functions needed for the adaptation to restricted growth or stress (high affinity ABC-type transporters, transcription regulators).

Below we will focus on a selected group of proteins that either showed the most dramatic changes in amount and/or were relevant to the observed phenotypes of the *lon* mutant. The set of proteins that are overrepresented in this strain are of particular interest as they represent potential natural substrates of the archaeal-type LonB protease.

3.2.1. *Lipid metabolism (LIP)*

Various enzymes involved in lipid metabolism changed their concentration on account to Lon deficiency, being phytoene synthase (PS) (HVO_2524) the most remarkable (50–57 fold increase) in both growth phases. PS is the key enzyme in carotenoid biosynthesis catalyzing the conversion of geranylgeranyl pyrophosphate (GGPP) to phytoene [38]. This step is conserved in all carotenogenic organisms, including haloarchaea [39]. At first glance it is surprising that PS was only detected in the membrane fraction as it is not predicted to contain transmembrane helices or potential motifs for lipid modifications that could account for membrane localization. The homologous protein found in plants does not have apparent membrane anchors, however, in tomato chloroplasts PS activity appears to be membrane-associated based on the requirement of high-ionic strength buffer or mild non-ionic detergent for its solubilization [40,41]. In chromoplasts of *Narcissus pseudonarcissus* (daffodil) PS occurs in two topologically distinct forms, one soluble in the stroma and the other tightly membrane-bound [40]. The soluble form is enzymatically inactive but gains activity when it is membrane-associated. However, the structural basis for PS membrane affinity is unclear as the deduced amino acid sequence does not exhibit membrane-spanning regions. Based on this evidence, the possibility that *H. volcanii* PS could be linked to the membrane by other means (a membrane protein or lipid head groups) cannot be ruled out.

The carotenoids biosynthetic pathway has been extensively characterized in plants [38] and it appears that PS is regulated by

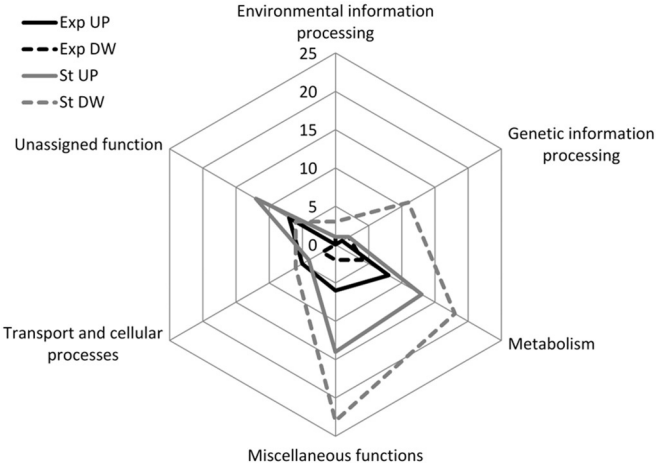

Fig. 2 – Proteins showing differential abundance between *H. volcanii* wt and *lon* deficient strains. Proteins were classified into functional categories and were distributed according to their relative amount (up, UP or down-regulation, DW) and growth phase (Exp or St). Numbers indicate number of proteins.

phytochrome-interacting factors at the transcript level [42]. PS is up-regulated in flowers during chromoplasts development and it was suggested that both transcriptional and post-translational mechanisms may account for color development [40].

In *Haloferax mediterranei* and *H. volcanii* bacterioruberin content changes depending on medium salinity [43,44]. In *H. mediterranei* and *Haloarcula hispanica* overexpression of the *ctrB* gene encoding PS produces cell overpigmentation while a knockout mutant renders the cultures colorless [45]. Our finding that the protein level of PS dramatically increases when Lon is down-regulated (Table 1) is consistent with the elevated bacterioruberin content observed in the Lon deficient cells, and conversely, the colorless phenotype produced by Lon overexpression [12]. Although additional experiments are necessary to confirm whether PS is degraded by LonB, our previous results and those presented in this study strongly suggest that LonB is a key factor in the regulation of carotenogenesis in haloarchaea.

Phospholipids are the major components of cellular membranes in all organisms. The current and limited information on phospholipid biosynthesis in archaea derives from methanogens while this pathway has been examined scarcely in other archaeal organisms. *In silico* analysis of complete genomes shows that archaea encode homologs of the enzymes involved in phospholipid biosynthesis in bacteria and eukaryotes [46]. In this proteomic study, phosphatidylserine decarboxylase (HVO_0146) changed substantially in the *lon* mutant (decreased in protein amount by 12-fold). This protein is predicted to be associated to the membrane (contains a transmembrane domain) and, by analogy to bacterial/eukaryal enzymes, it is expected to catalyze the conversion of archaetidylserine (AS) to archaetidylethanolamine (AE), the archaeal analogs of phosphatidylserine (PS) and phosphatidylethanolamine (PE), respectively [47].

Halobacterium sp NRC-1 and *Haloarcula marismourti* (and other haloarchaea including *H. volcanii*) encode homologs of archaetidylserine synthase (ASS) and archaetidylserine decarboxylase (ASD), however, the phospholipids AS and AE have not been identified in haloarchaea [48], leading to the conclusion that these enzymes may not be functional in these organisms. However, the fact that in this study ASS and ASD were detected at the protein level in *H. volcanii* (Supplemental Table S1 in [34]) and that ASD shows differential abundance in the *lon* mutant (Table 1) suggests that this may not be the case and thus, this issue is worthy of further investigation. Further analysis of the lipid composition of *H. volcanii* wt vs *lon* mutant would help to clarify whether ASD is functional in *H. volcanii*.

3.2.2. Co-enzyme metabolism (COM)

Several proteins involved in coenzyme metabolism were affected by Lon deficiency including those associated with biosynthesis of riboflavin, folate, molybdenum cofactor, ubiquinone, thiamine, NAD, and the porphyrin-derived compounds heme and vitamin B12 (cobalamin, CBL) (Table 1). Interestingly, there was a remarkable increase in the cellular content of various proteins related to vitamin B12 biosynthesis in exponentially growing Lon deficient cells. CBL is one of the most complex co-factors found in nature and it is synthesized only by a few prokaryotes, including bacteria and archaea [49,50]. CBL synthesis starting from uroporphyrinogen III can be accomplished by aerobic (*cob* genes) or anaerobic (*cbi/cob* genes) pathways which differ in the cobalt integration step. Haloarchaea encode both cobalt chelatases, the oxygen-dependent *cobN* and the oxygen independent *cbiX*. While haloarchaea encode most *cob* genes, some are absent, suggesting alternative reactions and enzymes for CBL synthesis [39]. Several proteins belonging to the same transcriptional unit (HVO_B0052 to HVO_B0062) increased significantly (1.5–27 fold) in the *lon* mutant (HVO_B0052, HVO_B0054, HVO_B0055, HVO_B0057, HVO_B0058, HVO_B0059 and HVO_B0062). Therefore, it appears that the complete transcriptional unit is regulated by Lon, probably by degradation of a transcriptional regulator. Other proteins participating in porphyrin metabolism also increased significantly in Lon-deficient cells (Table 2). Siroheme decarboxylase AhbA (HVO_2227), which participates in an alternative route for heme biosynthesis, showed a strong decrease of 35-fold. This could be due to competition for the same substrate, considering that AhbA uses the same precursor (precorrin 2) as the enzymes leading to CBL synthesis.

It is worth noting that some of the enzymes involved in CBL synthesis (HVO_A0487, HVO_B0051, HVO_B0052, HVO_B0058, HVO_B0059 and HVO_B0062) increased their concentration in

Table 2 – Proteins involved in CBL and heme biosynthesis affected by the *lon* mutation. Regulation factors for four biological replicates were submitted to a Student's t-test and p-values ≤ 0.05 were considered significant. Changes are expressed in fold (positive and negative numbers signify an increase or decrease in the mutant strain, respectively). FR, cellular fraction in which the protein was found to be differential (C: cytoplasm, M: membrane).

ID	FR	Gene name	Protein name	Fold Exp	*p*-value	Fold St	*p*-value
HVO_0081	C/M	*hemL*	glutamate-1-semialdehyde 2,1-aminomutase	1.2/1.7	0.003/0.036	1.2	0.030
HVO_A0487	C/M	*cbiA,cobB*	cobyrinic acid a.c-diamide synthase	1.7/11.4	0.004/0.030		
HVO_B0050	M	*cobN*	ATP-dependent cobaltochelatase subunit CobN	1.7	0.014	1.4	0.044
HVO_B0051	C/M	*hmcA*	ATP-dependent cobaltochelatase subunit ChlID	1.5/2.5	0.016/0.004		
HVO_B0052	C	-	PQQ repeat protein	2.9	0.007		
HVO_B0054	C	*cbiK*	sirohydrochlorin cobaltochelatase	9.8	0.013		
HVO_B0055	C	-	conserved hypothetical protein			2.0	0.031
HVO_B0057	M	*cbiH2,cobJ2*	precorrin-3B C17-methyltransferase	9.8	0.047		
HVO_B0058	C	*cbiH1,cobJ1*	precorrin-3B C17-methyltransferase	27	0.002		
HVO_B0059	C	*cbiG*	cobalt-precorrin 5A hydrolase	1.5	0.010		
HVO_B0062	C	*cbiT*	precorrin-7 15-methyltransferase (decarboxylating)			1.9	0.004
HVO_2227	C	*ahbAn nirDL*	siroheme decarboxylase AhbA			−35.6	

wt *H. volcanii* upon entrance into the St phase (Supplemental Table S1). This observation correlates with stabilization of these enzymes in the Lon-deficient cells during Exp growth.

In bacteria, Lon mediated proteolysis controls heme synthesis by degradation of HemA [51]. Our results suggest that Lon also controls the very complex biosynthetic route of these cofactors in *H. volcanii*.

3.2.3. Amino acid biosynthesis (AA)

Various enzymes involved in amino acid biosynthesis were affected in Lon-deficient St phase cells, mainly those leading to the synthesis of lysine, histidine and methionine (Table 1).

Methionine plays an important role in cellular metabolism as it is used in protein synthesis, methylation reactions, polyamine and N-acyl homoserine lactone biosynthesis. Two enzymes involved in methionine biosynthesis (HVO_2999, HVO_2946) were severely underrepresented in *H. volcanii* mutant cells. In *E. coli* methionine synthesis is partially regulated through degradation of homoserine trans-succinylase by the action of the ATP-dependent proteases Lon and Clp [52].

Several enzymes involved in the synthesis of lysine (HVO_1098, HVO_1099, and HVO_1100) showed a substantial increase in the *lon* mutant (Table 1). The opposite effect (down-regulation) was observed in the transition to St phase in wt cells (Supplemental Table S1). A decrease in lysine biosynthetic enzymes upon entrance into St phase was also reported for *Haloarcula marismortui* [53]. The fact that these genes form an operon suggests that the effect of Lon may be indirect, for instance, by degradation of a transcriptional regulator.

Based on this study, it appears that Lon also participates in the regulation of aa biosynthesis in archaea.

3.2.4. ABC-type transporters (TP)

The ATP-binding cassette (ABC) transporters constitute a primary transport system used to import/export substrates that is found in the three domains of life. The canonical ABC importers of prokaryotes consist of two transmembrane segments (TMS, translocation pore), two nucleotide binding domains facing the cytoplasm (NBDs, ATP binding and hydrolysis) and a substrate binding protein (SBP) localized in the periplasm or external surface of the cytoplasmic membrane [54]. ABC-type importers are used for the uptake of a wide variety of substrates including amino acids, peptides, sugars, vitamins and ions, thus, they function in energy supply, osmoregulation and virulence. Due to their high specificity and substrate affinity (kd 0.01–1 μM), these transporters are usually induced under stress conditions (e.g. St phase) facilitating scavenging trace amounts of substrates. In *H. volcanii* H26 wt several ABC-type transporters for amino acids, peptides and sugars were dramatically enriched up to 270 fold in St phase cells compared to exponentially growing cells (Supplemental Table S1). Interestingly, components of ABC-type transporters for organic (amino acids, peptides and sugars) as well as inorganic compounds (phosphorous, iron, copper) were differentially represented in the *lon* mutant (Table 1), some of which (HVO_0899; 2800; A0494 and B0021) corresponded to those that increased their concentration in St phase cells.

HVO_0899 and HVO_B0021 were underrepresented by 32 and 65 fold in St phase cells, while HVO_0627 and HVO_A0477 transporters for dipeptides and phosphate, respectively, were overrepresented by 83 and 15 fold in Exp Lon deficient cells. The differential impact (up or down-regulation) of the *lon* mutation on the relative concentrations of these proteins reflects that Lon may control the level of ABC-type transporters by different mechanisms such as degrading a transporter component (e.g. HVO_0627 and HVO_A0477) or, alternatively, a regulatory protein which may control (inhibit) their synthesis (HVO_0899 and HVO_B0021) in order to fit the physiological requirements of the cell under nutrient scarcity.

HVO_2163 (*lolD*) and HVO_2165 (*lolE*) encode homologs of the ATP-binding and permease components of the ABC transporter-like LolDCE. The Lol (lipoprotein outer membrane localization) pathway is involved in the selection, transport and insertion of lipoproteins to the outer membrane in Gram negative bacteria [55]. These homologs increased in the *lon* mutant by 2 to 7 fold and based on their genetic organization they seem to form an operon together with LolC.

3.2.5. Transcription regulators (REG)

Various proteins predicted to function as DNA-binding transcription regulators were affected in cells with suboptimal Lon expression. These include homologs of the Leucin-responsive Regulatory Protein Lrp/AsnC family (HVO_2858 and HVO_0179), ArsR family transcription regulator (HVO_1552); IcIR family (HVO_2108), a protein with DNA-binding HTH domain (HVO_2421) and a hypothetical protein encoding a ribbon-helix-helix regulator of the CopG family (HVO_0583).

Lrp/AsnC (HVO_2858) and the DNA binding protein encoded by HVO_2421 were overrepresented in the *lon* mutant (12 and 22 fold, respectively). On the contrary, ArsR and IcIR were underrepresented by 9 and 15 fold, respectively. The Lrp/AsnC regulators interact in different ways with DNA (repression or activation) and can function as master regulators or in a gene-specific manner affecting the expression of individual genes/operons. These transcription factors control several metabolic pathways in bacteria and archaea including amino acid biosynthesis and degradation, energy and central metabolism as well as transport systems [56]. For most of the Lrp/AsnC archaeal regulators the biological function and target genes are unknown. *Halobacterium salinarum* R1 encodes eight homologs of which Lrp and Lrp A1 were characterized [57]. These regulators influence amino acids and central metabolic pathways, transcriptional regulators as well as phosphate and peptide transporters.

The Ars and the IclR families of transcriptional regulators occur in bacteria and archaea and modulate the expression of genes directly associated with metal homeostasis [58] and genes involved in carbon metabolism [59], respectively.

Taking into account the global changes detected in the proteome of the *lon* mutant, including catabolic and biosynthetic enzymes, ABC-type transporters, proteins involved in carbon metabolism, it is possible that Lon exerts control of these cellular functions by modulating the protein level of these transcription regulators.

3.2.6. Protein secretion and processing (MIS)

Signal peptide peptidases (Spps) are transmembrane proteins that hydrolyse signal peptides from secretory proteins once they have been cleaved from the pre-protein by signal peptidases [13].

The cleaved fragments of signal peptides may be released from the membrane and function in signal transduction pathways both in eukaryotes and bacteria. SppA (Peptidase S49; Protease IV) is a serine protease that has a catalytic Ser-Lys dyad and it is found in all domains of life. HVO_1987 encodes a homologue of SppA and based on its genetic organization, it appears to form an operon with HVO_1988 which encodes a hypothetical protein related to peptidase S49/SppA. Interestingly, both proteins were dramatically enriched in both growth phases in response to Lon deficiency, especially during the St phase (78 and 122 fold for HVO_1987 and HVO_1988, respectively). Consistent with the topology of bacterial SPPs, these proteins contain a signal peptide, an additional transmembrane segment and most of the protein is predicted to face the periplasm. The current knowledge on this family of proteases is limited in archaea, and only a few enzymes derived from the thermophiles have been characterized [60–62]. Assuming that SppA exerts similar functions in archaeal cells, it can be speculated that by affecting the levels of SppAs Lon controls signaling pathways in haloarchaea. Moreover, it is worth noting that HVO_1988 gene product is one of the proteins most greatly affected by the *lon* mutation (122 fold increase, Table 1) suggesting it may play a relevant but so far unknown role *in vivo*.

3.2.7. Genetic processes (RMT, RRR, TC and TL)

Proteins involved in genetic processes that increased their concentration in the *lon* mutant included an SMC-like protein homolog, PCNA and an enzyme involved in RNA maturation (23S rRNA uridine- 2´-O-methyltransferase, FtsJ, HVO_0180).

The structural maintenance of chromosome protein superfamily (SMC) is widespread in eukaryotes and prokaryotes. SMC-like proteins are involved in various essential chromosome-related processes including DNA condensation, sister chromatid cohesion, recombination, DNA repair and dosage compensation. *H. salinarum* encodes two of such proteins, Sph1 and Sph2, of these Sph1 was previously characterized. Its expression is growth phase-dependent, both transcript and protein levels increase in growing cells and dramatically decrease in the St phase [63]. The means that control the level of Sph1 are uncertain. *H. volcanii* genome also encodes homologs of SMC-like proteins and the SMC-like protein Sph2 (HVO_B0118) was overrepresented by 2.3-fold in Lon deficient St phase cells. Although this change is modest, it would be consistent with a role of Lon in the regulation of DNA related processes upon entrance into the St phase through degradation of SMC-like proteins. In support of this hypothesis, in *Bacillus subtilis* members of this protein family are degraded by the ATP-dependent proteases Clp and LonA during the St phase [64].

PCNA, the processivity subunit of DNA polymerase, was reported to be stabilized in a proteasome mutant and later confirmed to be degraded by the proteasome in *H. volcanii* [65]. We observed that PCNA (HVO_0175) was enriched by 2 fold in St phase cells with suboptimal expression of Lon protease. This result suggests that these proteases may have partial overlapping functions to control the level of proteins involved in key cellular processes such as replication and DNA repair.

The 23S rRNA uridine-2′-O-methyl transferase FtsJ is responsible for the 2′-O-methylation of the universally conserved U2552 in the A loop of 23S rRNA. In *E. coli* this modification seems to be critical for ribosome stability as absence of functional FtsJ produces cellular accumulation of individual ribosomal subunits at the expense of functional 70S ribosomes [66]. By extrapolation, the increase of the FtsJ homologous enzyme in the *H. volcanii lon* mutant (12 fold) may account for the diminished concentration of free ribosomal subunits observed in this strain (Table 1). On the other hand this enzyme showed a significant increase (10 fold) in response to the transition from Exp to St phase, which could imply that Lon is responsible for the down-regulation of FtsJ in vegetative cells.

3.2.8. Various functions

In *H. volcanii*, proteasomes are composed of five different polypeptides denoted as α1, α2 and β which form at least two 20S proteasome subtypes (α1, α2, β) and (α1, β), and two different proteasome activating nucleotidase proteins; PAN-A and PAN-B [4]. The levels of the α2 subunit and PAN-B are growth phase-dependent (e.g. low levels are detected in lag to log phase while high levels are observed in St phase cells) suggesting that these proteins are associated in a common pathway [67]. In this work the proteasome α2-subunit (HVO_2923) was found to be overrepresented by 2 fold in the *lon* mutant in exponentially growing cells suggesting that Lon could be responsible for degradation of this proteasome component in vegetative cells, and thus, would control the cellular concentration of the (α1, α2, β) subtype proteasomes.

3.2.9. Proteins of unknown function (HY and CHY)

At least 22 proteins of unknown function, detected in both membrane and cytosol fractions, changed their concentration in the *lon* mutant and 17 were overrepresented. It is interesting to note that HVO_A0039 is the protein that showed the highest increase in amount in the *lon* mutant (321 and 95 fold in Exp and St phase, respectively). This protein contains a TMS and is predicted to be localized facing the periplasmic space, thus, it is possible that it may have a role on the cell surface. HVO_A0012, predicted to be a cytoplasmic protein, was increased 22-fold. Interestingly, these proteins are plasmid encoded and are present only in haloarchaea suggesting that they may play a rather specific, so far unknown role in these organisms (adaptation to high salt habitats?).

The hypothetical proteins represent interesting targets for future research as they may reveal proteins with novel functions and/or those involved in organism-specific adaptations to extreme environments.

3.3. Overlapping functions of LonB with archaeal proteasomes

Kirkland and co-workers have examined the effect of proteasomes on *H. volcanii* proteome composition. Total proteins extracted from cells incubated with the specific proteasome inhibitor clasto-lactacystin-B-lactone [23] or from a mutant strain deleted in the proteasome activating-nucleotidase PanA subunit (delta *panA*) [22] were fractionated by 2D-gel electrophoresis and identified by mass spectrometry techniques. These conditions affected the relative amounts and/or phosphorylation status of a large number of proteins that participate in a variety of cellular processes such as protein quality control, translation, cell division, solute transport and metabolism as

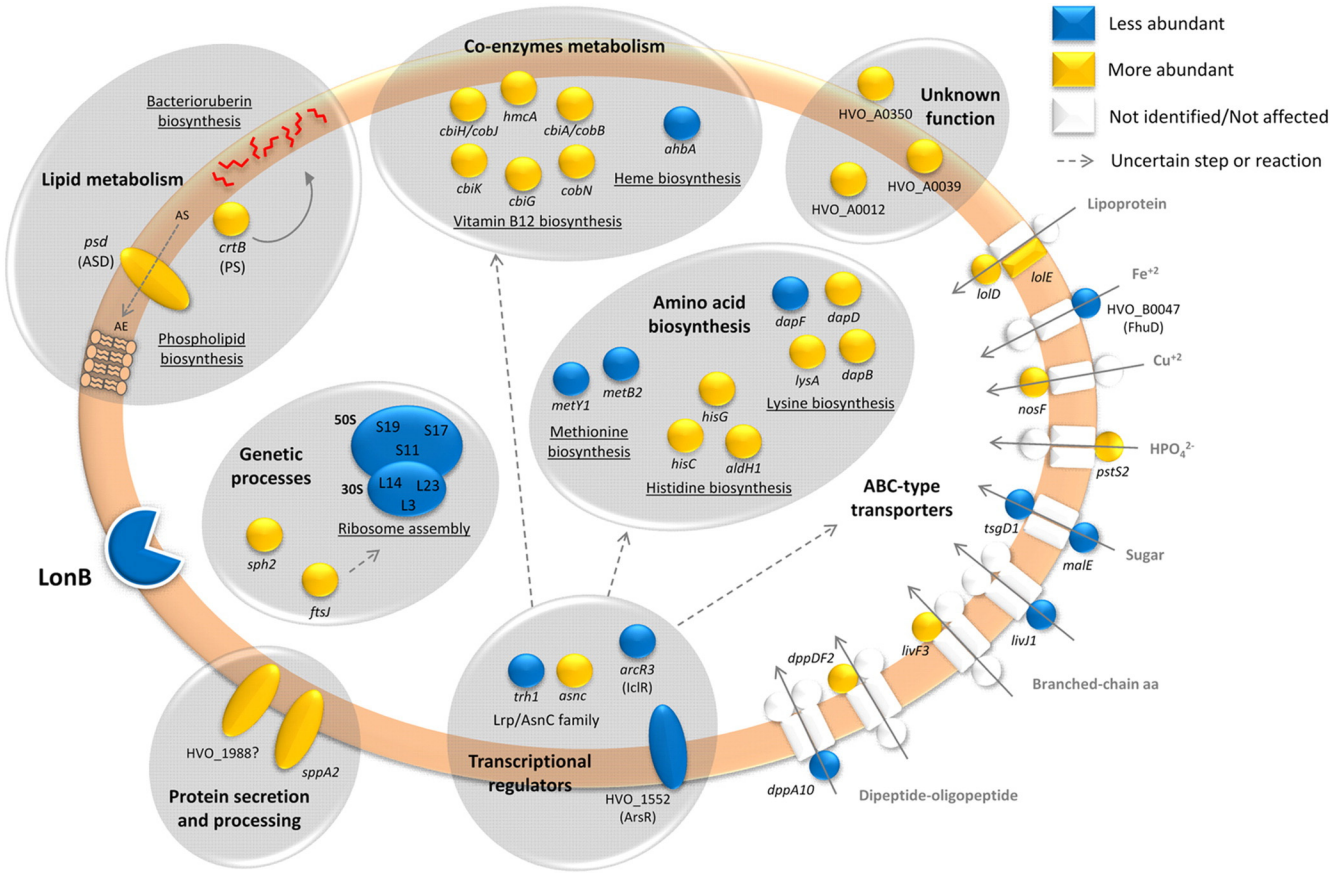

Fig. 3 – Schematic representation of the proteins and processes affected by Lon deficiency in *H. volcanii*. Proteins are identified by gene/protein names or locus tag. See text for details.

well as proteins of unknown function. The proteome examination of the *lon* conditional mutant shows that the LonB protease also affects key functions in archaeal cells. Based on comparison of the proteins affected in the proteasome [22,23,65] and Lon mutants (this study), only a few were detected as common "substrates". These include NAD-dependent epimerase/dehydratase (HVO_2040), PCNA and phytoene synthase. Thus, it appears that these ATP-dependent proteolytic complexes have little overlapping functions in archaea which is consistent with the lethal phenotype of mutations in either the proteasome or Lon in *H. volcanii*.

4. Conclusion

This study is the first proteome analysis of an organism deficient in the membrane-associated LonB protease. Similarly as in bacteria, LonB has a global impact on the physiology of the euryarchaeon *H. volcanii*, affecting key cellular processes as well as organism-specific so far unknown functions which may be required for survival/adaptation under extreme conditions. Fig. 3 shows a schematic representation of the proteins and cellular processes affected in the *lon* conditional mutant (down-regulation) in *H. volcanii*, this working model will guide future investigations aiming to address Lon function in archaea. The proteins enriched in the *lon* mutant (soluble and membrane-associated polypeptides) represent potential natural substrates of the membrane protease LonB. Thus, this work will help in the discovery of endogenous targets of the archaeal-type Lon as well as novel targets/processes regulated by Lon proteases. Complementary experiments, such as determination of global and/or specific protein turnovers, will help to address this issue.

Supplementary data to this article can be found online at http://dx.doi.org/10.1016/j.jprot.2015.03.016.

Transparency Document

The Transparency document associated with this article can be found, in the online version.

Acknowledgements

MC acknowledges EMBO and Boehringer-Ingelheim Fonds for financial support at Ruhr University Bochum, Germany. This work was supported by grants from CONICET (PIP 1783) and UNMDP (EXA 632/13) awarded to RDC and the joint project supported by MINCyT (AL/13/02, Argentina)-BMBF (01DN14007, Germany) awarded to RDC and AP. MC is a PhD student at the National University of Mar del Plata (Argentina) supported by a research fellow from CONICET. The authors thank Dr F. Pfeifer (Max Planck Institute, Martinsried, Germany) for providing the *H. volcanii* proteome dababase.

REFERENCES

[1] Sauer RT, Baker TA. AAA+ proteases: ATP-fueled machines of protein destruction. Annu Rev Biochem 2011;80:587–612.
[2] De Castro RE, Maupin-Furlow JA, Gimenez MI, Herrera Seitz MK, Sanchez JJ. Haloarchaeal proteases and proteolytic systems. FEMS Microbiol Rev 2006;30:17–35.
[3] Saeki Y, Tanaka K. Assembly and function of the proteasome. Methods Mol Biol 2012;832:315–37.
[4] Kaczowka SJ, Maupin-Furlow JA. Subunit topology of two 20S proteasomes from *Haloferax volcanii*. J Bacteriol 2003;185: 165–74.
[5] Zhou G, Kowalczyk D, Humbard MA, Rohatgi S, Maupin-Furlow JA. Proteasomal components required for cell growth and stress responses in the haloarchaeon *Haloferax volcanii*. J Bacteriol 2008;190:8096–105.
[6] Eichler J, Maupin-Furlow J. Post-translation modification in *Archaea*: lessons from *Haloferax volcanii* and other haloarchaea. FEMS Microbiol Rev 2013;37:583–606.
[7] Maupin-Furlow JA, Gil MA, Humbard MA, Kirkland PA, Li W, Reuter CJ, et al. Archaeal proteasomes and other regulatory proteases. Curr Opin Microbiol 2005;8:720–8.
[8] Tojo N, Inouye S, Komano T. Cloning and nucleotide sequence of the *Myxococcus xanthus lon* gene: indispensability of *lon* for vegetative growth. J Bacteriol 1993; 175:2271–7.
[9] Van Melderen L, Aertsen A. Regulation and quality control by Lon-dependent proteolysis. Res Microbiol 2009;160: 645–51.
[10] Pinti M, Gibellini L, Guaraldi G, Orlando G, Gant TW, Morselli E, et al. Upregulation of nuclear-encoded mitochondrial LON protease in HAART-treated HIV-positive patients with lipodystrophy: implications for the pathogenesis of the disease. Aids 2010;24:841–50.
[11] Breidenstein EB, Hancock RE. Armand-Frappier outstanding student award – role of ATP-dependent proteases in antibiotic resistance and virulence. Can J Microbiol 2013;59: 1–8.
[12] Cerletti M, Martinez MJ, Gimenez MI, Sastre DE, Paggi RA, De Castro RE. The LonB protease controls membrane lipids composition and is essential for viability in the extremophilic haloarchaeon *Haloferax volcanii*. Environ Microbiol 2014;16: 1779–92.
[13] Dalbey RE, Wang P, van Dijl JM. Membrane proteases in the bacterial protein secretion and quality control pathway. Microbiol Mol Biol Rev 2012;76:311–30.
[14] Weichart D, Querfurth N, Dreger M, Hengge-Aronis R. Global role for ClpP-containing proteases in stationary-phase adaptation of *Escherichia coli*. J Bacteriol 2003;185:115–25.
[15] Frees D, Andersen JH, Hemmingsen L, Koskenniemi K, Baek KT, Muhammed MK, et al. New insights into *Staphylococcus aureus* stress tolerance and virulence regulation from an analysis of the role of the ClpP protease in the strains Newman, COL, and SA564. J Proteome Res 2012;11:95–108.
[16] Major T, von Janowsky B, Ruppert T, Mogk A, Voos W. Proteomic analysis of mitochondrial protein turnover: identification of novel substrate proteins of the matrix protease *pim1*. Mol Cell Biol 2006;26:762–76.
[17] Solheim C, Li L, Hatzopoulos P, Millar AH. Loss of Lon1 in Arabidopsis changes the mitochondrial proteome leading to altered metabolite profiles and growth retardation without an accumulation of oxidative damage. Plant Physiol 2012;160: 1187–203.
[18] Gibellini L, Pinti M, Boraldi F, Giorgio V, Bernardi P, Bartolomeo R, et al. Silencing of mitochondrial Lon protease deeply impairs mitochondrial proteome and function in colon cancer cells. FASEB J 2014;28:5122–35.
[19] Ludke A, Kramer R, Burkovski A, Schluesener D, Poetsch A. A proteomic study of *Corynebacterium glutamicum* AAA+ protease FtsH. BMC Microbiol 2007;7:6.
[20] Chitlaru T, Zaide G, Ehrlich S, Inbar I, Cohen O, Shafferman A. HtrA is a major virulence determinant of *Bacillus anthracis*. Mol Microbiol 2011;81:1542–59.
[21] Westphal K, Langklotz S, Thomanek N, Narberhaus F. A trapping approach reveals novel substrates and physiological functions of the essential protease FtsH in *Escherichia coli*. J Biol Chem 2012;287:42962–71.
[22] Kirkland PA, Gil MA, Karadzic IM, Maupin-Furlow JA. Genetic and proteomic analyses of a proteasome-activating nucleotidase A mutant of the haloarchaeon *Haloferax volcanii*. J Bacteriol 2008;190:193–205.
[23] Kirkland PA, Reuter CJ, Maupin-Furlow JA. Effect of proteasome inhibitor clasto-lactacystin-beta-lactone on the proteome of the haloarchaeon *Haloferax volcanii*. Microbiology 2007;153:2271–80.
[24] Sastre DE, Paggi RA, De Castro RE. The Lon protease from the haloalkaliphilic archaeon *Natrialba magadii* is transcriptionally linked to a cluster of putative membrane proteases and displays DNA-binding activity. Microbiol Res 2010;166:304–13.
[25] Allers T, Ngo HP, Mevarech M, Lloyd RG. Development of additional selectable markers for the halophilic archaeon *H. volcanii* based on the *leuB* and *trpA* genes. Appl Environ Microbiol 2004;70:943–53.
[26] Dyall-Smith M. The Halohandbook: Protocols for haloarchaeal genetics; 2008 23[http://www.haloarchaea.com/resources/halohandbook/index.html].
[27] Dyballa N, Metzger S. Fast and sensitive colloidal coomassie G-250 staining for proteins in polyacrylamide gels. J Vis Exp 2009;30:1431.
[28] Schluesener D, Fischer F, Kruip J, Rogner M, Poetsch A. Mapping the membrane proteome of *Corynebacterium glutamicum*. Proteomics 2005;5:1317–30.
[29] Olsen JV, de Godoy LM, Li G, Macek B, Mortensen P, Pesch R, et al. Parts per million mass accuracy on an Orbitrap mass spectrometer via lock mass injection into a C-trap. Mol Cell Proteomics 2005;4:2010–21.
[30] Eng JK, McCormack AL, Yates JR. An approach to correlate tandem mass spectral data of peptides with amino acid sequences in a protein database. J Am Soc Mass Spectrom 1994;5:976–89.
[31] Dorfer V, Pichler P, Stranzl T, Stadlmann J, Taus T, Winkler S, et al. MS Amanda, a universal identification algorithm optimized for high accuracy tandem mass spectra. J Proteome Res 2014;13:3679–84.
[32] Pfeiffer F, Broicher A, Gillich T, Klee K, Mejía J, Rampp M, et al. Genome information management and integrated data analysis with HaloLex. Arch Microbiol 2008;190(3):281–99 [1. PubMed PMID: 18592220; PubMed Central PMCID: PMC2516542].
[33] Kall L, Storey JD, MacCoss MJ, Noble WS. Posterior error probabilities and false discovery rates: two sides of the same coin. J Proteome Res 2008;7:40–4.
[34] Cerletti M, Paggi RA, Ramallo Guevara C, De Castro RE. Data in soport of global role of the membrane protease LonB in *Archaea*: Potential protease targets revealed by quantitative proteome analysis of a *lonB* mutant in *Haloferax volcanii*. J Proteome Data in Brief 2015 [in press].
[35] Liu H, Sadygov RG, Yates 3rd JR. A model for random sampling and estimation of relative protein abundance in shotgun proteomics. Anal Chem 2004;76: 4193–201.
[36] Haussmann U, Qi SW, Wolters D, Rogner M, Liu SJ, Poetsch A. Physiological adaptation of *Corynebacterium glutamicum* to benzoate as alternative carbon source – a membrane proteome-centric view. Proteomics 2009;9:3635–51.

[37] Fischer F, Poetsch A. Protein cleavage strategies for an improved analysis of the membrane proteome. Proteome Sci 2006;4:2.
[38] Shumskaya M, Wurtzel ET. The carotenoid biosynthetic pathway: thinking in all dimensions. Plant Sci 2013;208:58–63.
[39] Falb M, Muller K, Konigsmaier L, Oberwinkler T, Horn P, von Gronau S, et al. Metabolism of halophilic archaea. Extremophiles 2008;12:177–96.
[40] Schledz M, al-Babili S, von Lintig J, Haubruck H, Rabbani S, Kleinig H, et al. Phytoene synthase from *Narcissus pseudonarcissus*: functional expression, galactolipid requirement, topological distribution in chromoplasts and induction during flowering. Plant J 1996;10:781–92.
[41] Fraser PD, Schuch W, Bramley PM. Phytoene synthase from tomato (*Lycopersicon esculentum*) chloroplasts–partial purification and biochemical properties. Planta 2000;211:361–9.
[42] Toledo-Ortiz G, Huq E, Rodriguez-Concepcion M. Direct regulation of phytoene synthase gene expression and carotenoid biosynthesis by phytochrome-interacting factors. Proc Natl Acad Sci U S A 2010;107:11626–31.
[43] D'Souza SE, Altekar W, D'Souza SF. Adaptive response of *Haloferax mediterranei* to low concentrations of NaCl (<20%) in the growth medium. Arch Microbiol 1997;168:68–71.
[44] Bidle KA, Hanson TE, Howell K, Nannen J. HMG-CoA reductase is regulated by salinity at the level of transcription in *Haloferax volcanii*. Extremophiles 2007;11:49–55.
[45] Liu H, Han J, Liu X, Zhou J, Xiang H. Development of *pyrF*-based gene knockout systems for genome-wide manipulation of the archaea *Haloferax mediterranei* and *Haloarcula hispanica*. J Genet Genomics 2011;38:261–9.
[46] Daiyasu H, Kuma K, Yokoi T, Morii H, Koga Y, Toh H. A study of archaeal enzymes involved in polar lipid synthesis linking amino acid sequence information, genomic contexts and lipid composition. Archaea 2005;1:399–410.
[47] Schuiki I, Daum G. Phosphatidylserine decarboxylases, key enzymes of lipid metabolism. IUBMB Life 2009;61:151–62.
[48] Corcelli A, Lobasso S. Characterization of lipids of halophilic archaea. In: Rainey AF, Oren A, editors. Methods in microbiology. Amsterdam: Academic Press/Elsevier Inc.; 2006. p. 585–613.
[49] Rodionov DA, Vitreschak AG, Mironov AA, Gelfand MS. Comparative genomics of the vitamin B12 metabolism and regulation in prokaryotes. J Biol Chem 2003;278:41148–59.
[50] Kang Z, Zhang J, Zhou J, Qi Q, Du G, Chen J. Recent advances in microbial production of delta-aminolevulinic acid and vitamin B12. Biotechnol Adv 2012;30:1533–42.
[51] Wang L, Elliott M, Elliott T. Conditional stability of the HemA protein (glutamyl-tRNA reductase) regulates heme biosynthesis in *Salmonella typhimurium*. J Bacteriol 1999;181:1211–9.
[52] Biran D, Gur E, Gollan L, Ron EZ. Control of methionine biosynthesis in *Escherichia coli* by proteolysis. Mol Microbiol 2000;37:1436–43.
[53] Chu LJ, Yang H, Shih P, Kao Y, Tsai YS, Chen J, et al. Metabolic capabilities and systems fluctuations in *Haloarcula marismortui* revealed by integrative genomics and proteomics analyses. J Proteome Res 2011;10:3261–73.
[54] Eitinger T, Rodionov DA, Grote M, Schneider E. Canonical and ECF-type ATP-binding cassette importers in prokaryotes: diversity in modular organization and cellular functions. FEMS Microbiol Rev 2011;35:3–67.
[55] Zuckert WR. Secretion of bacterial lipoproteins: through the cytoplasmic membrane, the periplasm and beyond. Biochim Biophys Acta 1843;2014:1509–16.
[56] Peeters E, Charlier D. The Lrp family of transcription regulators in archaea. Archaea 2010;2010:750457.
[57] Schwaiger R, Schwarz C, Furtwangler K, Tarasov V, Wende A, Oesterhelt D. Transcriptional control by two leucine-responsive regulatory proteins in *Halobacterium salinarum* R1. BMC Mol Biol 2010;11:40.
[58] Osman D, Cavet JS. Bacterial metal-sensing proteins exemplified by ArsR-SmtB family repressors. Nat Prod Rep 2010;27:668–80.
[59] Zhang RG, Kim Y, Skarina T, Beasley S, Laskowski R, Arrowsmith C, et al. Crystal structure of *Thermotoga maritima* 0065, a member of the IclR transcriptional factor family. J Biol Chem 2002;277:19183–90.
[60] Matsumi R, Atomi H, Imanaka T. Biochemical properties of a putative signal peptide peptidase from the hyperthermophilic archaeon *Thermococcus kodakaraensis* KOD1. J Bacteriol 2005;187:7072–80.
[61] Matsumi R, Atomi H, Imanaka T. Identification of the amino acid residues essential for proteolytic activity in an archaeal signal peptide peptidase. J Biol Chem 2006;281:10533–9.
[62] Kocabiyik S, Demirok B. Cloning and overexpression of a thermostable signal peptide peptidase (SppA) from *Thermoplasma volcanium* GSS1 in *E. coli*. Biotechnol J 2009;4:1055–65.
[63] Herrmann U, Soppa J. Cell cycle-dependent expression of an essential SMC-like protein and dynamic chromosome localization in the archaeon *Halobacterium salinarum*. Mol Microbiol 2002;46:395–409.
[64] Mascarenhas J, Volkov AV, Rinn C, Schiener J, Guckenberger R, Graumann PL. Dynamic assembly, localization and proteolysis of the *Bacillus subtilis* SMC complex. BMC Cell Biol 2005;6:28.
[65] Kirkland PA, Maupin-Furlow JA. Stabilization of an archaeal DNA-sliding clamp protein, PCNA, by proteasome-activating nucleotidase gene knockout in *Haloferax volcanii*. FEMS Microbiol Lett 2009;294:32–6.
[66] Hager J, Staker BL, Jakob U. Substrate binding analysis of the 23S rRNA methyltransferase RrmJ. J Bacteriol 2004;186:6634–42.
[67] Reuter CJ, Kaczowka SJ, Maupin-Furlow JA. Differential regulation of the PanA and PanB proteasome-activating nucleotidase and 20S proteasomal proteins of the haloarchaeon *Haloferax volcanii*. J Bacteriol 2004;186:7763–72.
[68] Oliveros JC. VENNY. An interactive tool for comparing lists with Venn Diagrams. 2007 [http://bioinfogp.cnb.csic.es/tools/venny/index.html].